Electronic charge redistribution in $LaAlO_3$(001) thin films deposited at $SrTiO_3$(001) substrate: predictions from first principles

A. Sorokin[1], S. Piskunov[1,2,3], D. Bocharov[1,2,3], V. Kashcheyevs[1,2,3]

[1]Faculty of Physics and Mathematics, University of Latvia, Zellu 8, LV-1002 Riga, Latvia, [2]Faculty of Computing, University of Latvia, Raina blvd., LV-1586 Riga, Latvia, [3]Institute of Solid State Physics, Kengaraga 8, LV- 1063 Riga, Latvia. E-mail of presenting author: bocharov@latnet.lv

Motivation

Thin film heterostructures containing the two simple band insulators $LaAlO_3$ (LAO) and $SrTiO_3$ (STO) have recently attracted a wide attention because of their intriguing properties, which include a quasi two-dimensional conducting electron gas, low temperature superconductivity, and magnetism. These properties are not present in the parent bulk materials. In order to understand this novel behavior it is necessary to discover an approach capable to describe the way how these heterostructures deal with the polar discontinuity at the interface.

Thickness of LAO(001) deposited atop STO(001) substrate is the most critical characteristic responsible for insulator/conductor transition in LAO/STO. Results calculated to date show that for n-type interfaces such a transition occurs due to polar distortion if thin film is thicker than 5 u.c. However depending on experimental conditions (pressure/temperature) n-type heterostructures can be found either insulating without any respect to film thickness or exhibit conductance at thickness of 2 u.c. assuming that oxygen vacancies and cation intermixing play a major role. p-type interface remains insulating independently on thin film thickness while from "polar catastrophe" approach it is predicted to show a hole conductance.

Our contribution

Using two different LCAO and PW calculation methods, in this contribution we simulate from first principles plane-by-plane epitaxial growth of LAO(001) thin film atop STO(001). Calculated electron charge redistribution at the interface allows us to provide deeper insight into the origin of its conductivity.

An extensive set of the literature can be found in these two nice reviews:

1.R. Pentcheva and W.E. Pickett, J. Phys.: Condens. Matter 22 (2010) 043001

2.H. Chen, A.M. Kolpak, S. Ismail-Beigi, Adv. Mater. 22 (2010) 2881

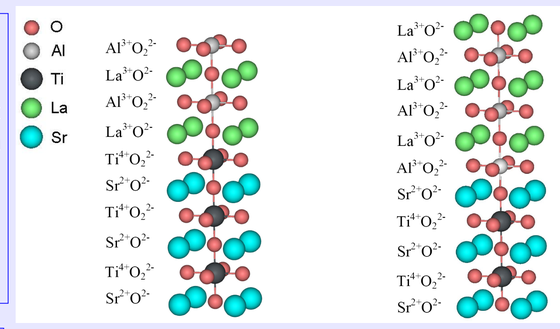

Fig. 1. Schematic representation of ↑ LAO/STO(001) heterostructures of (left) n-type and (right) p-type.

Results: $LaAlO_3/SrTiO_3$(001)

For n-type LAO/STO(001) it always exhibits n-type conductance if it is LaO-terminated. For AlO_2-term. heterostructures conductance occurs if LAO(001) nanofilm is at least 5 (4 in VASP) u.c. thick (in agreement with polar distortion mechanism proposed by Pentcheva and Pickett, PRL 102, 107602 (2009)).

Our calculations show that if e.g. 4 unit cell of LAO thin film are deposited atop STO substrate, ~0.5e is located in LaO contact interface plane. This charge is compensated by -0.5e (hole) placed at AlO_2-terminated surface plane in agreement with previous theoretical predictions. However, if the same LAO(001) thin film is LaO-terminated, surface plane acquire additionally ~0.2e thus giving rise to conductance. For similar thin film interface but of p-type, -0.5e is transfered to AlO2 interface contact plane while charge of 0.5e is found to be located in LaO-terminated surface plane. -0.3e is located in AlO2-terminated surface plane of potentially conducting p-type LAO/STO interface. (Fig. 4, 5, 6).

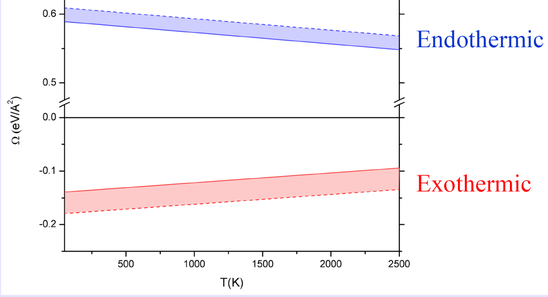

Fig.2. Calculated thermodynamic stability diagram of LAO(001) with respect to precipitation of La and Al metallic phases, O liquid phase, and formation of La_2O_3 and Al_2O_3 oxides atop surfaces. →

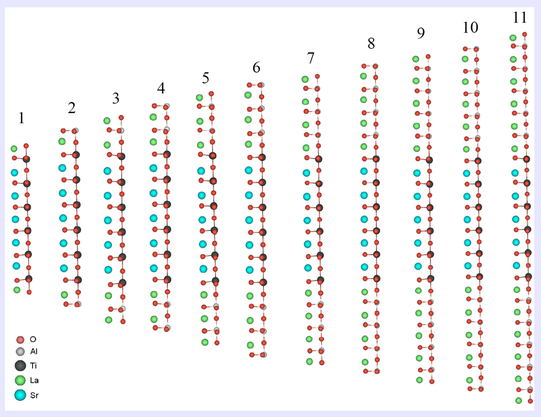

Fig. 3. Slab unit cells of LAO/STO(001) heterostructures we have considered in our study. These all are n-type structures. The same set of p-type heterostructures has been also considered. ←

Results: $LaAlO_3$(001)

9-plane LAO(001) slabs of both LaO- and AlO_2-terminations have been considered. In agreement with Tang et al. Physics Letters A 365 (2007) 149–155 we predict n-type conductance for LaO-term. LAO(001) and p-type conductance for AlO_2-term. LAO(001). (Fig. 7, 8).

Table I. Band gaps of LAO/STO(001) heterostructures under consideration as calculated by means of both PW and LCAO computational schemes.

Nr. of planes STO-LAO-STO	n-type:	CR'09	VASP 5	p-type:	CR'09	VASP 5
	Termination	Gap, eV	Gap, eV	Termination	Gap, eV	Gap, eV
1-11-1	LaO-	Cond.	Cond.	AlO_2-	Cond.	Cond.
2-11-2	AlO_2-	3.65	1.41	LaO-	4.00	1.60
3-11-3	LaO-	Cond.	Cond.	AlO_2-	Cond.	Cond.
4-11-4	AlO_2-	2.91	1.03	LaO-	4.05	1.69
5-11-5	LaO-	Cond.	Cond.	AlO_2-	Cond.	Cond.
6-11-6	AlO_2-	1.96	0.40	LaO-	4.05	1.51
7-11-7	LaO-	Cond.	Cond.	AlO_2-	Cond.	Cond.
8-11-8	AlO_2-	1.07	0.03 (Cond*)	LaO-	3.80	0.48 (0.26*)
9-11-9	LaO-	Cond.	Cond.	AlO_2-	Cond.	Cond.
10-11-10	AlO_2-	Cond.	Cond. (Cond*)	LaO-	2.92	0.10 (0.25*)
11-11-11	LaO-	Cond.	Cond.	AlO_2-	Cond.	Cond.
	LAO bulk gap:	5.81 eV	3.18 eV	5.6 eV exp.		
	STO bulk gap:	3.98 eV	1.77 eV	3.2 eV exp.		

* 8-13-8 and 10-13-10 VASP calculations

Fig. 4. $LaAlO_3/SrTiO_3$(001) of n-type: PDOS by CRYSTAL code ↓

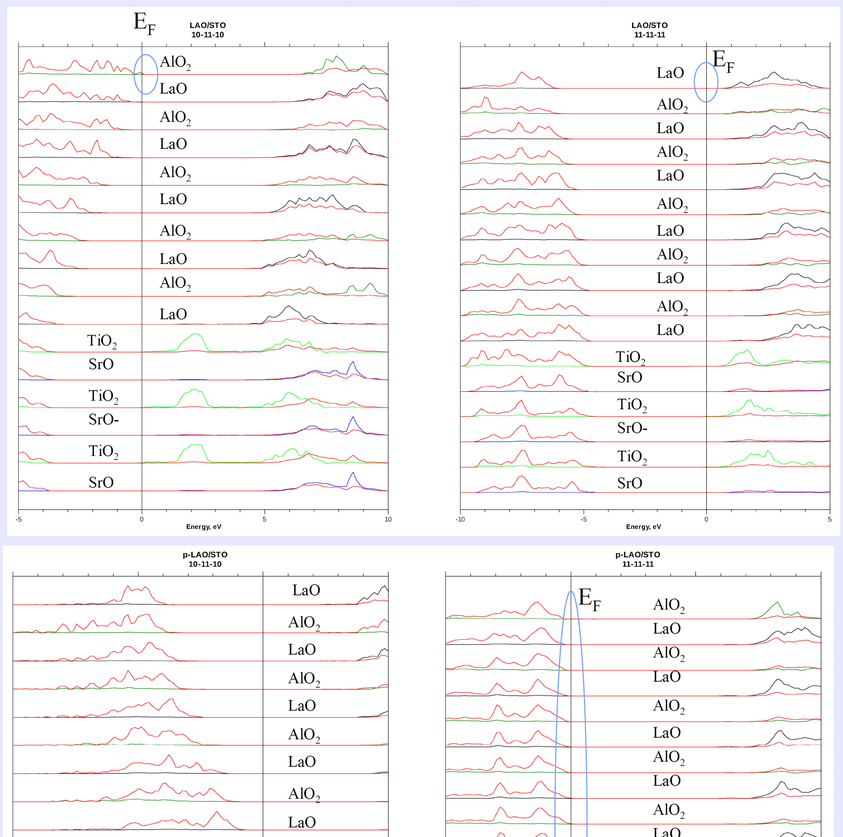

Fig. 5. $LaAlO_3/SrTiO_3$(001) of p-type: PDOS by CRYSTAL code ↑

Fig. 6. $LaAlO_3/SrTiO_3$(001) of n-type: PDOS by VASP code ↓

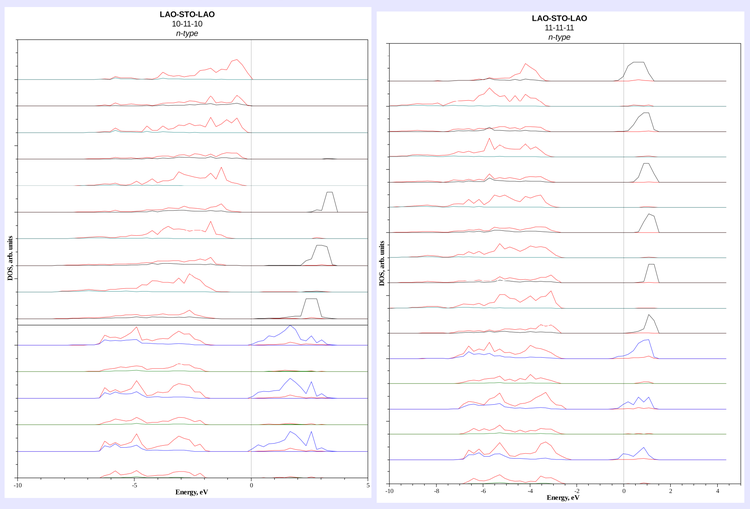

↑ *Fig. 7.* Pure $LaAlO_3$ 9-layer slab with different terminations PDOS by CRYSTAL code

Fig. 8. Pure $LaAlO_3$ 9-layer slab with different terminations TOTAL DOS by VASP code →

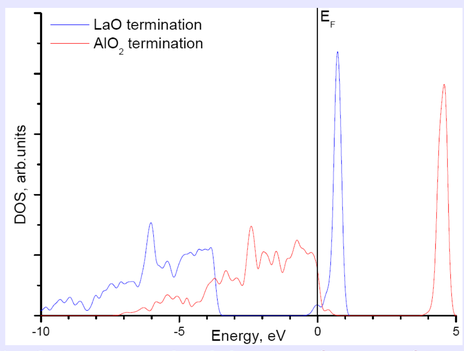

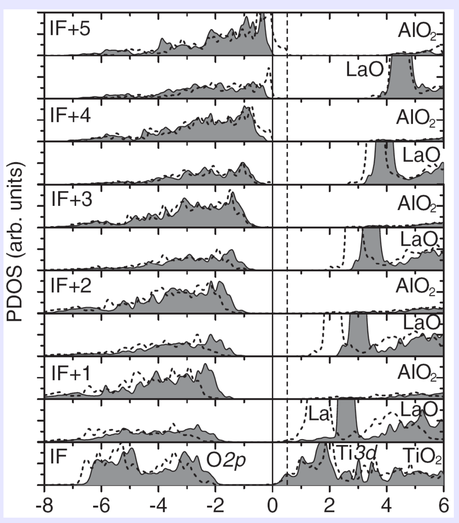

Fig. 9. Layer-resolved density of states of 5 multilayer of LAO on STO (001) n-type with ideal (dashed line) and relaxed (grey shaded area) coordinates from R. Pentcheva and W.E. Pickett PRL 102, 107602 (2009) paper. The DOS for ideal positions was shifted by 0.5 eV to align with the conduction band of the system with the relaxed atomic positions. Its Fermi level is marked with a dashed line. ←

Calculated thermodynamic stability diagram

LaO-terminated LAO(001) is predicted to be the most thermodynamically stable. (Fig. 2).

The most stable surface composition is the one which minimize the surface free energy:

$$\Omega(T,p)=\frac{1}{2A}\left[G^{slab}(T,p,N_i)-\sum_i N_i\mu_i(T,p)\right]$$

G^{slab} – Gibbs free energy of the surface structure, N – number of atoms in the slab, μ – chemical potential, A – slab surface area.

Gibbs surface free energy of LAO(001):

$$\Omega(T,p)=\frac{1}{2A}\left[G^{slab}-N_{La}\gamma^{bulk}_{LaAlO_3}(T,p)-(N_{Al}-N_{La})\mu_{Al}(T,p)-(N_O-3N_{La})\mu_O(T,p)\right]$$

Gibbs free energy of perovskite formation:

$$\Delta G_f^{LaAlO_3}(T,p)=\gamma^{bulk}_{LaAlO_3}(T,p)-\gamma^{bulk}_{La}(T,p)-\gamma^{bulk}_{Al}(T,p)-\frac{3}{2}E^{O_2}_{tot}(T,p)$$

Allowed range of chemical potentials with respect to decompositions to elements:

$$\Delta G_f^{LaAlO_3}(T,p)<\mu_{Al}(T,p)-\gamma^{bulk}_{Al}(T,p)<0\ ;\ \frac{1}{3}\Delta G_f^{LaAlO_3}(T,p)<\mu_O(T,p)-\frac{1}{2}E^{O_2}_{tot}<0$$

Allowed range of chemical potentials with respect to decompositions to La_2O_3 and Al_2O_3:

$$2\Delta G_f^{LaAlO_3}-\Delta G_f^{La_2O_3}<2\Delta\mu_{Al}+3\Delta\mu_O<\Delta G_f^{Al_2O_3}$$

Calculated Gibbs free formation energy of perovskites(oxides):

$\Delta G_f^{LaAlO_3}$ = -17.68 eV

$\Delta G_f^{La_2O_3}$ = -17.52 eV *vs.* 18.55 eV in experiment

$\Delta G_f^{Al_2O_3}$ = -16.68 eV *vs.* 17.37 eV in experiment

More details about this method see in Reuter and Scheffler, PRB 65 (2001) 035406

Table II. Calculated by CRYSTAL code Mulliken effective net charge per plane with respect to the bulk.

	n-type	Cond.		p-type	Cond.
LaO	**Cond.**	**0.19**	AlO_2-	**Ins.**	**-0.28**
AlO_2-	-0.26	-0.50	LaO	0.08	0.45
LaO	0.44	0.45	AlO_2-	-0.38	-0.38
AlO_2-	-0.44	-0.48	LaO	0.43	0.42
LaO	0.47	0.48	AlO_2-	-0.39	-0.38
AlO_2-	-0.46	-0.48	LaO	0.39	0.41
LaO	0.47	0.49	AlO_2-	-0.38	-0.38
AlO_2-	-0.46	-0.47	LaO	0.38	0.42
LaO	0.48	0.49	AlO_2-	-0.38	-0.38
AlO_2-	-0.47	-0.46	LaO	0.38	0.46
LaO	0.52	0.44	AlO_2-	-0.42	-0.38
TiO_2-	0.04	0.06	SrO	-0.12	-0.01
SrO	-0.05	-0.05	TiO_2-	0.02	0.02

Summary

Our calculations predict that LaO-term LAO(001) is thermodynamically the most stable surface. LaO-term. LAO(001) is a typical n-type conductor while AlO_2-term. LAO(001) exhibits conductance of p-type. If LaO-term. LAO(001) nanofilm is deposited atop STO(001) substrate we predict n-type conductance for n-type heterointerfaces. In case of AlO_2-term. LAO(001) nanofilm deposited atop STO(001) insulator/conductor switching occurs due to polar distortion if nanofilm is at least 5 u.c. thick (n-type). LaO-term. p-type LAO/STO(001) remains insulating, while AlO_2-term. p-type heterointerface is always p-type conductor.

Computational details

As the first method *CRYSTAL-09* computer code based on the Gaussian-type functions centered on the atomic nuclei as the basis sets (BSs) for expansion of the linear combination of atomic orbitals (LCAO) has been used. We adopted here the hybrid B3PW exchange-correlation functional within the density-functional theory DFT. The BSs used in this study for both STO and LAO and LMO bulk computations were taken in the following forms: for Sr – 311d1G, Ti – 411d311G, O – 8–411d1G, Al – 8-621d1G, La –311-31d3f1 have been taken from CRYSTAL's homepage. For Al and O, all electrons are explicitly included. The inner core electrons of Sr and Ti are described by small-core Hay-Wadt effective pseudopotentials, but for La by the nonrelativistic pseudopotential created by Dolg *et al.* The reciprocal space integration was performed by sampling the Brillouin zone (BZ) with the 8x8x1 Pack-Monkhorst mesh. The cutoff threshold parameters of CRYSTAL for Coulomb and exchange integrals evaluation (ITOL1–ITOL5) have been set to 8, 8, 8, 8, and 16, respectively. Calculations were considered as converged only when the total energy obtained in the self-consistency procedure differs by less than 10^{-7} a.u. in two successive cycles.

As the second method the DFT-PW computer code *VASP 5* based on the use of a plane wave basis set was applied. The Monkhorst-Pack scheme with 8×8×1 *k*-point meshes for slab and 8×8×8 for bulk in the BZ was used. The cut-off energy has been chosen to be 520 eV. The non-local exchange-correlation functional Perdew-Wang-91 using the generalized gradient approximation (GGA) was employed. Scalar relativistic PAW pseudopotentials in our calculations contain 11 valence electrons for La ($5s^25p^65d^16s^2$), 3 electrons ($3s^23p^1$) for Al, 10 electrons ($4s^24p^65s^2$) for Sr, 12 electrons ($3s^23p^63d^24s^2$) for Ti, and 6 electrons ($2s^22p^4$) for O, respectively. The vacuum gap was taken equal to 31.3 Å .

During geometry optimization all atoms in slab unit cell have been allowed to relax.

This study was partially supported by ESF project ESF project No. 2009/0216/1DP/1.1.1.2.0/09/APIA/VIAA/044.